MESSENGER GAMMA RAY SPECTROMETER AND EPITHERMAL NEUTRON HYDROGEN DATA REVEAL COMPOSITIONAL DIFFERENCES BETWEEN MERCURY'S HOT AND COLD POLES.

Jack T. Wilson[1], David J. Lawrence[1], Patrick N. Peplowski[1], and William C. Feldman[2]. [1]The Johns Hopkins University Applied Physics Laboratory, Laurel, MD 20723, USA; [2]Planetary Science Institute, Tucson, AZ (Jack.Wilson@jhuapl.edu).

The presence of hydrogen (H), most likely in the form of water ice, is well established in Mercury's permanently shaded polar craters. But lower concentrations that may exist away from the poles have not previously been well constrained. We have used data from the MErcury Surface, Space ENvironment, GEochemistry, and Ranging (MESSENGER) Gamma-Ray and Neutron Spectrometer to produce a map of the absolute H abundance in Mercury's northern hemisphere. We find a mean abundance of $400 \pm {}^{250}_{150}$ ppm and a latitudinal trend that agrees with earlier results showing enhanced hydrogen contained within Mercury's radar bright craters. Additionally, we observe a middle- and low-latitude variation in H abundance that is strongly correlated with maximum temperature 20 cm beneath Mercury's surface.

Introduction: Since the early 1990s, it has been thought that water ice is present in the permanently shadowed craters at Mercury's poles. The data returned by MESSENGER [1] have strengthened the association between the PSRs and water ice. At the north pole, neutron measurements from MESSENGER's Gamma-Ray and Neutron Spectrometer revealed the presence of H-rich material that is consistent with the presence of 50–100 wt% water ice within Mercury's north polar PSRs [2].

Lawrence et al. (2013) [2] made use of intermediate-energy, epithermal neutrons, which provide a sensitive measure of the bulk H abundances of near-surface planetary materials. They are produced by nuclear spallation reactions when galactic cosmic rays (GCRs) collide with nuclei in planetary surfaces. H atoms have a strong effect on the flux of epithermal neutrons due to their ability to moderate neutrons, a consequence of the similarity in mass between the neutron and H nucleus. Moderate amounts of H variability (i.e., a few hundred parts per million H) can cause detectable variations in epithermal neutrons.

In addition to neutron measurements, gamma-ray measurements can provide information about H abundances. This is usually accessed via the 2,223-keV gamma-ray line associated with the inelastic collision of neutrons with H nuclei. However, due to the low abundance of H on Mercury, an alternative route, first demonstrated in [3], is required. Here the ratio of gamma-ray lines produced from inelastic collision and neutron-capture processes from a single element is combined with knowledge of the total macroscopic neutron absorption cross section (Σ_a) to estimate the H abundance. Maps have been published of both the MESSENGER thermal neutron data [4] and the inferred Σ_a.

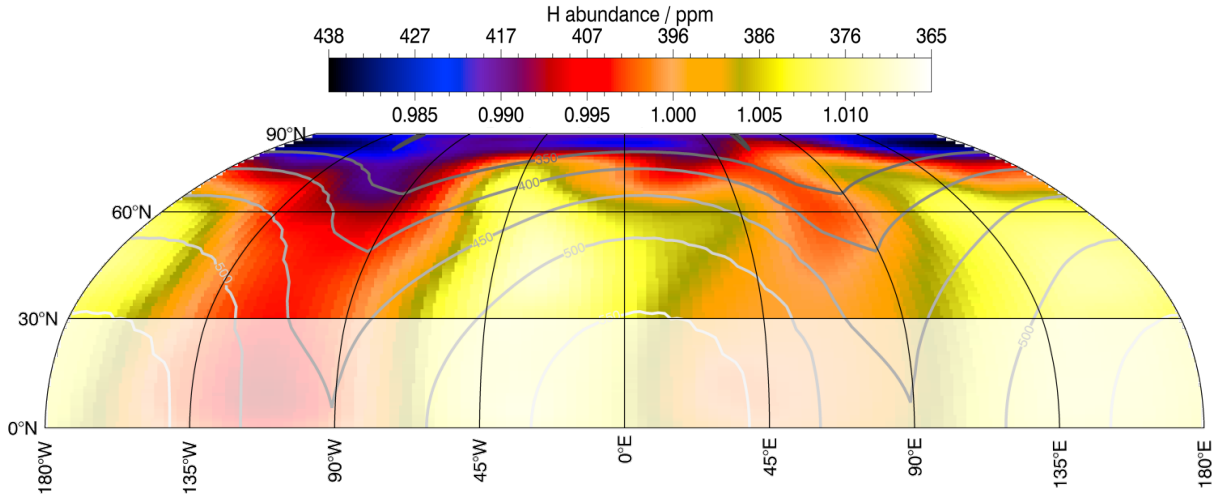

Figure 1: Northern hemisphere Robinson projection showing the smoothed epithermal flux with a conversion to H abundance in parts per million (ppm) based on GRS results and particle transport modelling. The greyed out region south of 30° N highlights the low signal to noise ratio data. The contours show maximum temperature at 20 cm depth.

Data and Methods: All five years of MESSENGER GRS and epithermal data measured by the borated plastic sensor are used in this study. This large dataset provides sufficient statistical precision to produce a robust map of the epithermal neutron flux.

The data reduction is detailed in [5]. Empirical corrections were made for variations in GCR flux, spacecraft attitude and solid angle subtended by the planet. Additionally, a correction was made for the Doppler-induced count rate variation based on the spacecraft velocity. This correction was unimportant for the fast neutron data but is important for the epithermal neutron data as the lower energy epithermal neutrons have a speed comparable to that of the spacecraft. As in [3] the efficacy of these corrections was verified by performing similar corrections on a mock data set to determine the size of residual systematic errors.

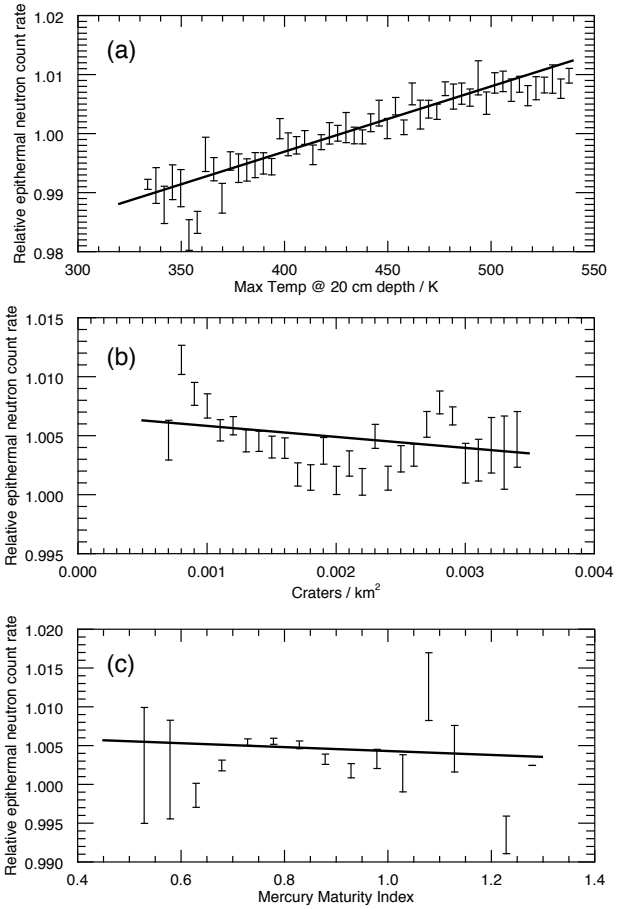

Figure 2: Plots of (a) maximum surface temperature, (b) crater density and (c) Mercury Maturity Index against corrected measured epithermal neutron count rate normalized to a mean of one. The plots are restricted to latitudes between 30° and 60° N to avoid the effects of the polar hydrogen deposits and low-SNR region close to the equator.

Results: Figure 1 shows the mapped, corrected epithermal neutron data. The absolute northern hemisphere average H abundance was determined from the GRS data to be $400 \pm {}^{250}_{150}$ ppm. The conversion from neutron flux to H abundance was based on the GRS result and particle transport modeling. As expected, the flux is low at the north pole implying an increased abundance of H and consistent with the presence of water ice in the permanently shaded craters. Significant additional variation is seen at equatorial to mid latitudes. Antipodal highs in epithermal flux are seen at ~30°W and ~150°E, which corresponds approximately to Mercury's hot poles as shown by the contours in Figure 1.

The correlation between near-surface temperature and epithermal neutron counts in the midlatitudes is shown clearly in Figure 2a. A strong positive trend is seen in the data, which corresponds to decreasing H abundance with increasing temperature. The correlation between temperature and epithermal neutron flux was found to be strongest for the maximum temperature at 20-cm depth, the mean depths from which neutrons originate (with Pearson correlation coefficient of 0.6 ± 0.02 compared with 0.5 ± 0.02 for correlation with surface temperature).

Correlation between epithermal flux and other parameters is weak. Figures 2b and 2c show the variation in neutron flux with crater density and Mercury Maturity Index, which are both proxies for surface age. Taken together these correlations seem to imply that the thermal stability effects outweigh the effect of increasing solar wind implantation with time.

Acknowledgments: The data used in this study are available from the Planetary Data System at pds-geosciences.wustl.edu/missions/messenger/ns_edr.html and grs_edr.html.

References: [1] Solomon, S. C., R. L. McNutt Jr., R. E. Gold, and D. L. Domingue, (2007) *Space Sci. Rev.*, 131, 3–39. [2] Lawrence, David J. et al (2013), *Science*, 339, 292-296. [3] Peplowski, Patrick N. et al. (2015), *Meteoritics and Planetary Science*, 50(3), 353–367. [4] Peplowski, Patrick N. et al. (2015) Icarus, 253, 346–363. [5] Wilson, Jack T. et al. (2019), *JGR*, 124, 721-733.